

Effects of Microstructure and Composition on the Curie Temperature of Lead Barium Niobate Solid Solutions

Takuya Hiroshima, Kazuhiko Tanaka, and Toshio Kimura*

Faculty of Science and Technology, Keio University, Yokohama 223 Japan

The Curie temperature of normally sintered and hot-pressed $Pb_{1-x}Ba_xNb_2O_6$ ($x = 0.30, 0.37, 0.41$, and 0.50) was dependent on the sample preparation conditions. Samples with large amounts of pores and cracks had higher Curie temperatures than dense samples. Dense samples with fine grains had higher Curie temperatures than those with coarse grains. Comparison between microstructure and the Curie temperature revealed that the variation in Curie temperature was caused by internal stresses developed in the paraelectric-to-ferroelectric phase transition. Large internal stresses increased the free energy of the ferroelectric phase, and thus decreased the Curie temperature. The magnitude of internal stresses depended on the microstructure. Pores and cracks relaxed internal stresses, resulting in high Curie temperatures. Grain boundaries also relaxed internal stresses; samples with small grains had high Curie temperatures. Furthermore, the magnitude of internal stresses was dependent on the crystal structure of ferroelectric phases; samples with the tetragonal ferroelectric structure had internal stresses larger than those with the orthorhombic ferroelectric structure. The effect of crystal structure was discussed in terms of the relaxation of internal stresses by the formation of 90° domains.

I. Introduction

THE Curie temperature of polycrystalline ferroelectric ceramics with a tungsten bronze structure is not uniquely determined by the composition, but depends on the sample preparation conditions, such as sintering conditions and heat treatment temperature.^{1–4} The variation in the Curie temperature has also been reported for single crystals quenched from various temperatures.^{5–7} Cation ordering^{2,6,7} and internal stresses^{3,4} have been proposed as the origin of the variation in the Curie temperature.

Guo *et al.*⁶ observed variation in the Curie temperature of up to about 40°C for strontium barium niobate single crystals annealed at various temperatures. They attributed the origin of the variation to the ordering of Sr and Ba ions. The tungsten bronze structure has five kinds of cation sites, A1, A2, B1, B2, and C. For strontium barium niobate, Nb ions occupy B1 and B2 sites, Ba and Sr ions occupy A1 and A2 sites, and C sites are vacant. The ordering of Ba and Sr ions in A1 and A2 sites, which is dependent on the temperature, determines the Curie temperature. Since cation ordering is dependent on the annealing temperature, the Curie temperature is dependent on the annealing temperature.

Another explanation for the variation in the Curie temperature is based on internal stresses.^{3,4} The transition from paraelectric (tetragonal, $4/mmm$) to ferroelectric phases (tetragonal, $4mm$ or orthorhombic, $mm2$) occurs during cooling⁸ when the

free energy of the ferroelectric phase becomes smaller than that of the paraelectric phase. The grain shape changes by the phase transition; the crystal surfaces perpendicular to the c -axis of the paraelectric phase move outward and those parallel to the c -axis move inward.^{9,10} If internal stresses associated with the shape change do not develop during the phase transition, the phase transition occurs at the normal Curie temperature. When the motion of crystal surfaces is impeded by the surrounding grains, internal stresses develop.¹¹ Internal stresses increase the free energy of the ferroelectric phase and decrease the Curie temperature. The fact that the Curie temperature is dependent on the preparation conditions of the samples^{1,3,4} indicates that the magnitude of internal stresses depends on the microstructure.

This paper deals with the effect of microstructure and composition on the Curie temperature of lead barium niobate solid solutions, $Pb_{1-x}Ba_xNb_2O_6$, with various x values to determine the origin of the variation in the Curie temperature in polycrystalline ceramics. Lead barium niobate has been selected because it is a ferroelectric material with the tungsten bronze structure and two crystal structures are present in the ferroelectric phase, orthorhombic ($x < 0.37$) and tetragonal ($x > 0.37$).¹² The effect of crystal structure of ferroelectric phase on the Curie temperature variation can be examined in this system.

II. Experimental Procedure

Chemically pure $BaCO_3$ (Yoneyama Chemical, Osaka, Japan), PbO (Kanto Chemical, Tokyo, Japan), and Nb_2O_5 (Shin-Etsu Chemical, Tokyo, Japan) powders were used as starting materials. The powders were mixed in a ball mill for 24 h using ethanol as a medium and then dried at 80°C for 24 h. Four batches with $x = 0.30, 0.37, 0.41$, and 0.50 were prepared. The mixed powders were pressed under a pressure of 16 MPa and then calcined at 1200°C for 2 h. Evaporation of PbO was prevented by covering the compacts with the powders of the same composition. The formation of single-phase solid solutions was confirmed by X-ray diffraction analysis. The calcined compacts were crushed and ground for 3 h in a planetary ball mill using a ZrO_2 container and ZrO_2 balls with a diameter of 15 mm. The ground powders were divided into two portions. One portion (powder C) was used for further experiments. The average particle sizes were about $1.4 \mu\text{m}$ for all compositions as determined by the centrifugal sedimentation method (CAPA-500, Horiba, Tokyo, Japan). The other portion (powder F) was further ground in a ball mill for 24 h to obtain powders with submicrometer particle sizes.¹³ For this grinding, a plastic container and ZrO_2 balls with a diameter of 2 mm were used. The average particle sizes were about $0.5 \mu\text{m}$ for all compositions.

The sintered compacts were made by normal sintering and hot pressing. For normal sintering, powders C and F were pressed under a pressure of 98 MPa, and the compacts were heated to desired temperatures at a heating rate of $180^\circ\text{C}/\text{h}$, soaked for 1 h, and then cooled in the furnace. The compacts were covered with the powders of the same composition to prevent PbO evaporation. For hot pressing, powders C were pressed under a pressure of 74.8 MPa. A calcined MgO powder was filled between the compact and the die to prevent PbO evaporation. Three hot-pressing programs (Fig. 1) were used.

Roy W. Rice—contributing editor

Manuscript No. 192074. Received January 23, 1996; approved June 14, 1996.
Supported by the Murata Science Foundation.
*Member, American Ceramic Society.

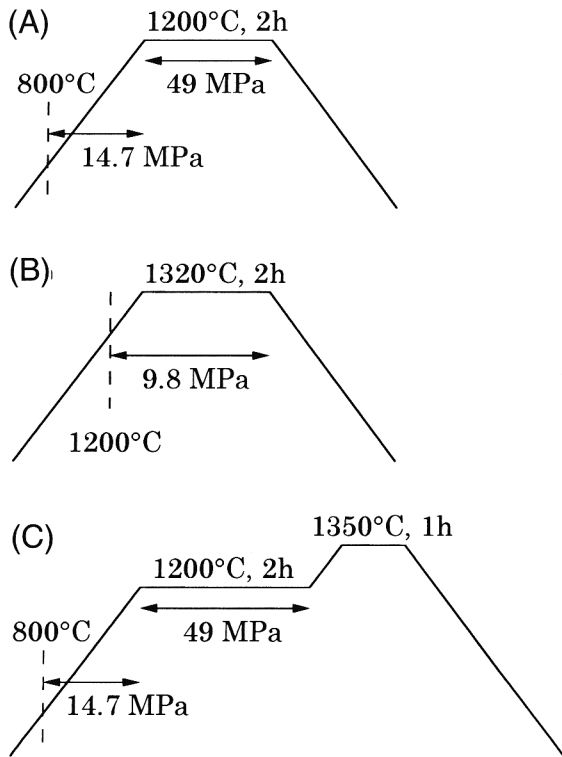


Fig. 1. Temperature–pressure programs (A) I, (B) II, and (C) III in hot pressing.

In each program, the heating rate was 270°C/h and the sample was cooled in the furnace.

X-ray diffraction (XRD) analysis using CuK α radiation (DX-GOP, JEOL, Tokyo, Japan) was used for the identification of phases and the measurement of lattice parameters; the diffraction angles of (350), (042), and (620) for the orthorhombic structure and (410), (221), and (311) for the tetragonal structure were measured for the lattice parameter determination. The density of sintered and hot-pressed compacts was measured by the Archimedes method, using water. The theoretical densities were determined from the lattice parameters of powders C; they were 6.34, 6.30, 6.22, and 6.14 for $x = 0.30$, 0.37, 0.41, and 0.50, respectively. The microstructure was observed on polished and thermally etched sections by scanning electron microscopy (SEM) (JSM-T100, JEOL, Tokyo, Japan). The

average grain size was obtained by the intercept method, where the average chord length of approximately 200 grains was multiplied by a factor of 1.5.¹⁴ The accuracy is estimated to be about 10%. The temperature dependence of relative permittivity was obtained from the measurement of capacitance at 1 kHz with an LCR meter (KG-536, Kokuyo Denki, Tokyo, Japan) at a heating rate of 150°C/h.

The magnitude of internal stresses was measured by the microindentation method.¹⁵ In this method, the fracture toughness K_{IC} is obtained from the length of an indentation crack ($2c$) using the equation

$$K_{IC} = 0.0726P/c^{3/2} \quad (1)$$

where P is the applied load. When a sample contains internal stresses, the effective fracture toughness K_{IC} is determined from the intrinsic fracture toughness K_{IC}^0 and the magnitude of internal stresses σ_i from the following equation.

$$K_{IC} = K_{IC}^0 + 2(c/\pi)^{1/2} \sigma_i \quad (2)$$

The magnitude of internal stresses was obtained from the slope of K_{IC} vs $c^{1/2}$ plot.

III. Results and Discussion

(1) Density and Microstructure

Figure 2 shows the effect of firing temperature on the relative density of compacts made by normal sintering. The densification behavior of powders C was almost the same for four compositions. For powders F, the densification behavior was almost the same for the samples with $x = 0.37$, 0.41, and 0.50, but the sample with $x = 0.30$ had poor sinterability. The origin of the poor sinterability of powder F with $x = 0.30$ will be discussed referring to the microstructure development (Fig. 5). Comparison of sintering behavior between powders C and F with the same composition indicates that powders F had better sinterability than powders C, except for the sample with $x = 0.30$. The small particle size of powders F is responsible for the better sinterability.¹³

Figure 3 shows the effect of firing temperature on the microstructure of sintered compacts with $x = 0.50$ made by normal sintering of powder C. Necks developed between particles, and the average grain sizes were about 3 and 4 μm for the samples sintered at 1200° and 1250°C, respectively. Extensive grain growth with the development of grain boundaries occurred above 1300°C. The average grain sizes were about 6 and 10 μm for the samples sintered at 1300° and 1350°C, respectively. Almost the same microstructural features were observed for

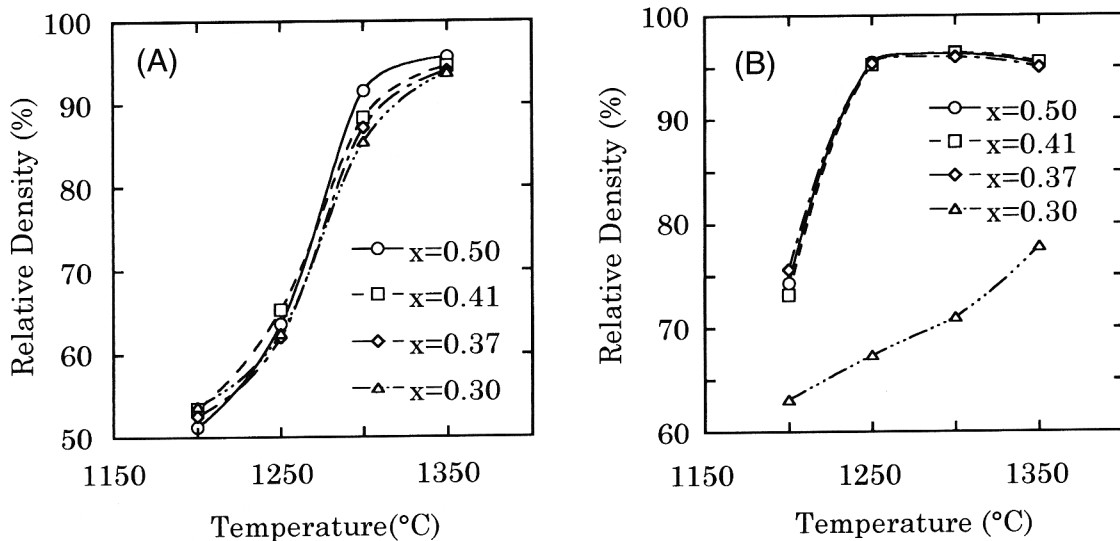


Fig. 2. Effect of firing temperature on the relative density of samples made by normal sintering of (A) powder C and (B) powder F.

other samples with x values different from 0.50 made by normal sintering of powders C.

Figure 4 shows the effect of firing temperature on the microstructure of sintered compacts with $x = 0.50$ made by normal sintering of powder F. At 1200°C, the grain size was smaller than that of the sample made from powder C (Fig. 3(A)). Dense structure with small grains developed at 1250°C. Abnormal grain growth occurred at 1300° and 1350°C. In these samples, extremely large grains and small grains coexisted. Furthermore, cracks developed in these samples. The presence of large grains is responsible for the formation of cracks; cracking begins when grain size exceeds a critical value.^{16–18} The samples with $x = 0.37$ and 0.41 made by normal sintering of powders F had the same microstructural features.

Different microstructure development was observed in the samples with $x = 0.30$ made by normal sintering of powder F (Fig. 5). Large grains formed at 1200° and 1250°C, as compared with other samples made from powders F (Fig. 4(A)). Many intragrain pores formed at this stage. Abnormal grain growth was not observed at 1300° and 1350°C, but grain growth was extensive and large intragrain pores formed. The formation of intragrain pores is responsible for the poor sinterability of this sample (Fig. 2(B)).

The relative densities of samples made by hot pressing of powders C were between 97% and 99% of theoretical. Figure 6 shows the microstructures of the samples with $x = 0.5$ obtained under three hot-pressing conditions shown in Fig. 1. The grain size increased as the maximum temperature of the hot-pressing program increased. The same microstructural features were observed for other samples with x values different from 0.5.

(2) Curie Temperature

Figure 7 shows the temperature dependence of relative permittivity of the samples with $x = 0.5$ made by normal sintering of powder C at various temperatures. The densities and microstructures of these samples are shown in Figs. 2(A) and 3, respectively. The relative permittivity increased as the firing temperature increased, for which the decrease in pore volume is responsible (Fig. 2(A)). Furthermore, the Curie temperature, defined as the temperature giving a maximum relative permittivity, decreased as the firing temperature increased. The same features were observed for other samples with x values different from 0.5 made by normal sintering of powders C.

Figure 8 shows the temperature dependence of relative permittivity of the samples with $x = 0.5$ made by normal sintering of powder F at various temperatures. The densities and microstructures of these samples are shown in Figs. 2(B) and 4, respectively. The relative permittivity was minimum and maximum for the samples fired at 1200° and 1250°C, respectively. Unlike the samples made from powder C (Fig. 7), the relative permittivity decreased as the firing temperature increased from 1250° to 1300° and 1350°C. The density of the samples fired at 1300° and 1350°C was slightly smaller than that of the sample fired at 1250°C, but the difference was not so significant (Fig. 2(B)). The presence of cracks is probably responsible for the reduction in relative permittivity for the samples fired at 1300° and 1350°C. The Curie temperature was also dependent on the firing temperature. Unlike the samples made from powder C (Fig. 7), the Curie temperature was maximum and

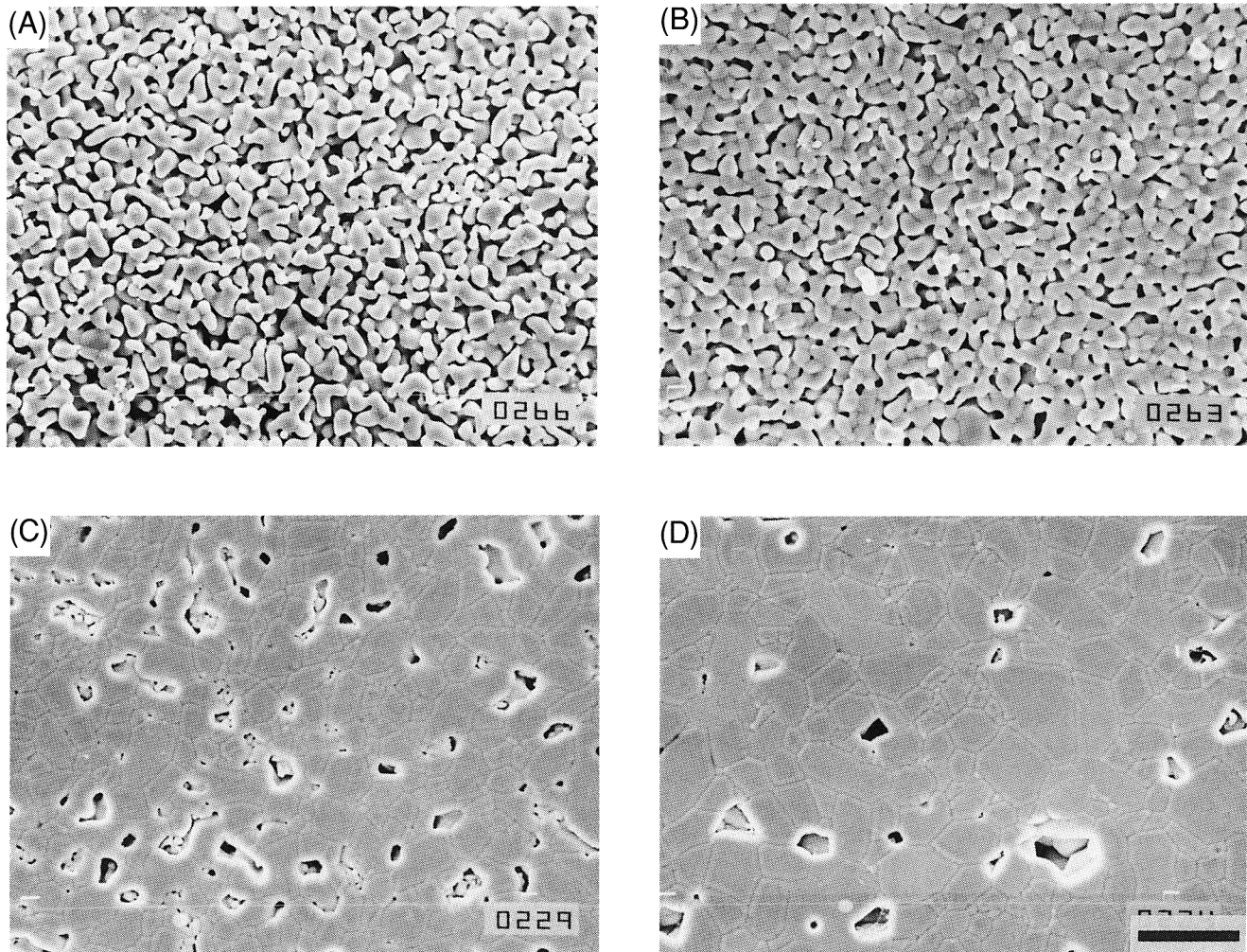


Fig. 3. Microstructures of the samples with $x = 0.50$ made by normal sintering of powder C at (A) 1200°, (B) 1250°, (C) 1300°, and (D) 1350°C for 1 h (bar = 20 μm).

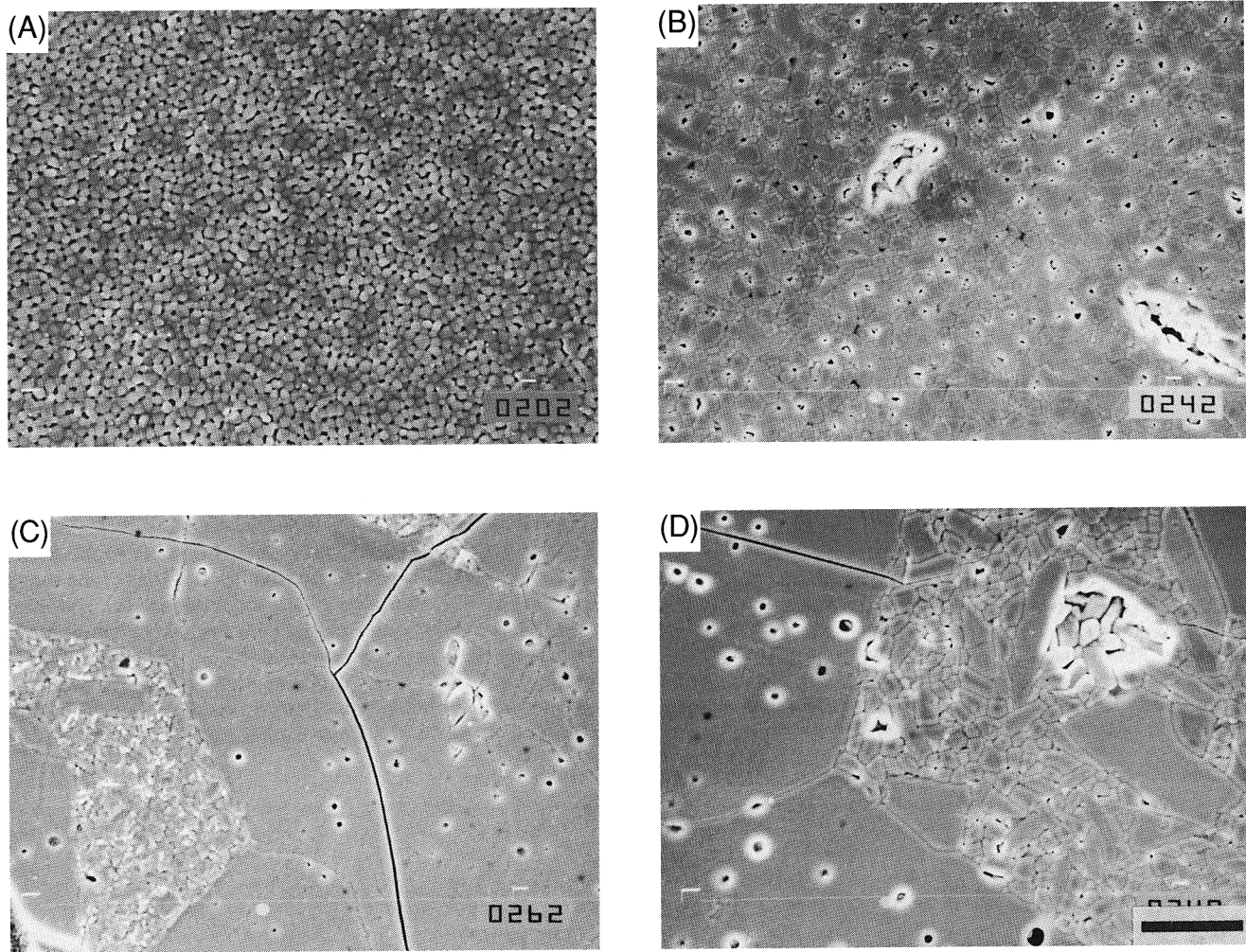


Fig. 4. Microstructures of the samples with $x = 0.50$ made by normal sintering of powder F at (A) 1200°, (B) 1250°, (C) 1300°, and (D) 1350°C for 1 h (bar = 20 μm).

minimum for the samples fired at 1200° and 1250°C, respectively. An increase in the firing temperature above 1300°C resulted in an increase in the Curie temperature from that of the sample fired at 1250°C. The same features were observed for other samples with $x = 0.37$ and 0.41 made by normal sintering of powders F.

The samples with $x = 0.30$ made by normal sintering of powder F had different features. Figure 9 shows the temperature dependence of relative permittivity of the samples fired at various temperatures. In this case, relative permittivity and the Curie temperature were not largely dependent on the firing temperature.

Figure 10 shows the temperature dependence of relative permittivity of the samples with $x = 0.50$ made by hot pressing of powder C. Three samples had almost the same relative permittivity, because these samples had almost the same density. The Curie temperature decreased as the maximum temperature of the hot-pressing program increased, i.e., as the grain size increased (Fig. 6). The same features were observed for other samples with x values different from 0.5.

(3) Origin of the Variation in the Curie Temperature

The variation in the Curie temperature of ferroelectrics with the tungsten bronze structure has been reported for several systems.^{1–7} The origins of the variation proposed in the literature are cation ordering^{2,6,7} and internal stresses,^{3,4} as mentioned in the Introduction.

The cation ordering model cannot be applicable to the explanation of the present results. The samples made by normal sintering of powders C and F had the same heating and cooling

program for the same firing temperatures, so that the cation ordering in the samples made from powders C and F with the same composition should be the same. However, the Curie temperatures of the samples fired at the same temperatures were different, as shown in Figs. 7 and 8. For example, the Curie temperatures of the samples with $x = 0.5$ made by normal sintering of powders C and F at 1300°C were 159° and 182°C, respectively. This indicates that the cation ordering cannot explain the variation in the Curie temperature for the samples with the same composition fired at the same temperature.

Another explanation is based on the internal stresses. Internal stresses develop in constrained grains at the phase transition temperature.¹¹ Internal stresses can be relieved by pores and cracks, because pores and cracks do not constrain grains. A decrease in the Curie temperature with an increase in firing temperature for the samples made by normal sintering of powder C (Fig. 7) can be explained by the presence of pore. The samples fired at 1200° and 1250°C were porous (Figs. 3(A) and (B)) so that the magnitude of internal stresses was small. The samples fired at 1300° and 1350°C were dense (Figs. 3(C) and (D)), resulting in large internal stresses. An increase in the magnitude of internal stresses decreases the Curie temperature.¹⁹

Another example of the effect of pores on the Curie temperature is illustrated by the sample with $x = 0.30$ made from powder F. These samples were porous and contained intragrain pores (Fig. 5). The Curie temperatures of these samples were almost the same, irrespective of the firing temperature (Fig. 9). The Curie temperatures of the samples with $x = 0.30$ made from powder C had dependence on the firing temperature similar to that shown in Fig. 7. Thus, the pore volume determines

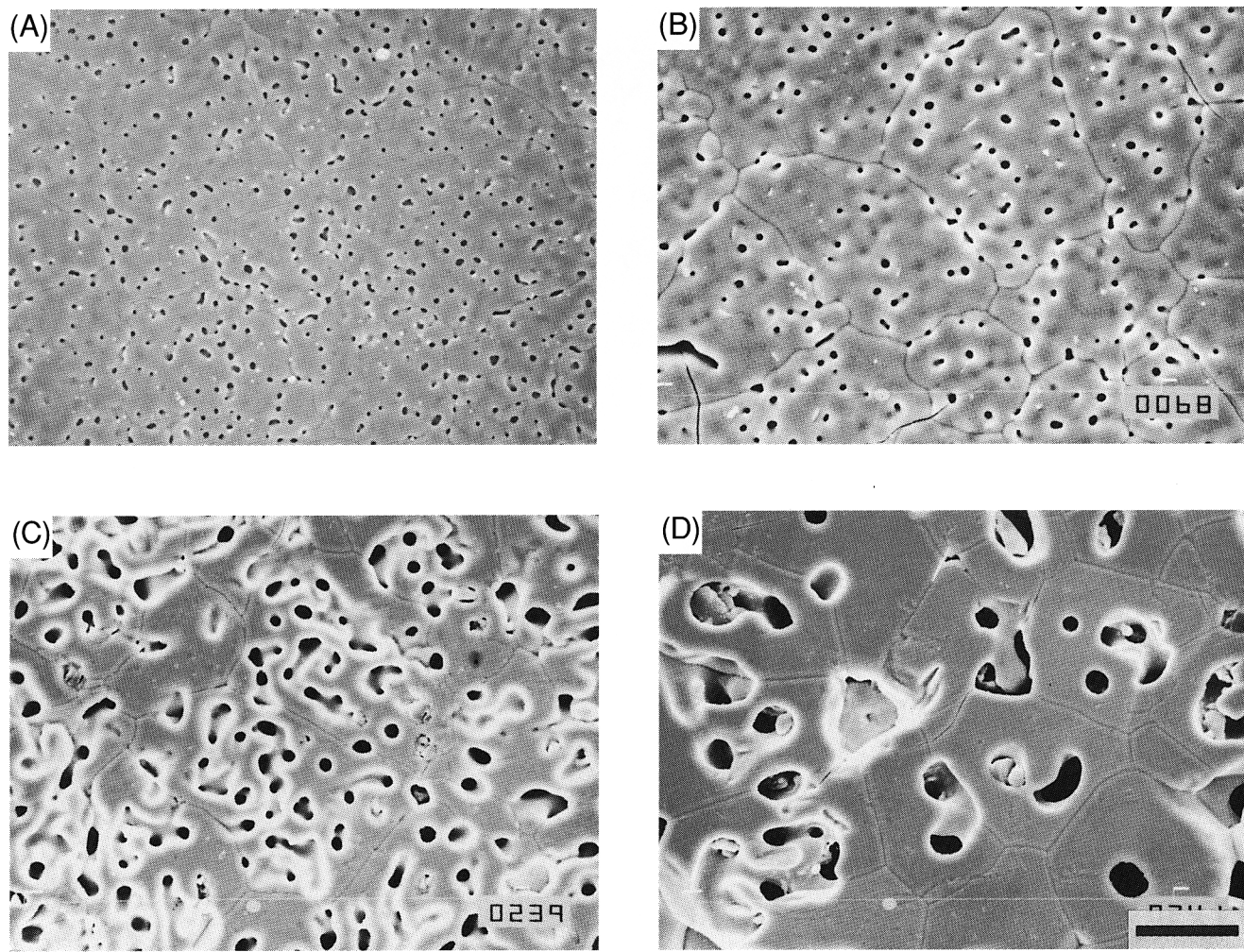


Fig. 5. Microstructures of the samples with $x = 0.30$ made by normal sintering of powder F at (A) 1200°, (B) 1250°, (C) 1300°, and (D) 1350°C for 1 h (bar = 20 μm).

the magnitude of internal stresses and the Curie temperature. The cracks also reduce the internal stresses. The effect of cracks is exemplified referring to the samples made from powder F at 1300° and 1350°C (Figs. 4(C) and (D)). These samples had Curie temperatures higher than that of the sample fired at 1250°C (Fig. 8) without cracks (Fig. 4(B)).

The effect of grain size on the Curie temperature is exemplified referring to the samples made by hot pressing (Figs. 6 and 10). The samples had small amounts of pores and also no cracks, because the grain sizes were less than the critical size for cracking. Thus, the relaxation of internal stresses by pores and cracks did not occur. Comparison between Figs. 6 and 10 indicates that the sample with the lower Curie temperature had larger grains (Fig. 6). The effect of grain size on the Curie temperature is explained as follows. Internal stresses are relieved by grain boundary sliding, and they are easily relieved in samples with large grain boundary areas. Thus, samples with fine grains have higher Curie temperatures than those with coarse grains.

(4) Measurement of Internal Stresses

The presence of internal stresses in the samples was verified by the measurements of lattice parameters and K_{1c} .

The crystal structure at room temperature was tetragonal for the samples with $x = 0.41$ and 0.50 and orthorhombic for the samples with $x = 0.30$ and 0.37, consistent with the reported phase diagram.¹² Figure 11 shows the relation between the axial ratio (c/a and b/a for the tetragonal and orthorhombic structures, respectively) and the Curie temperature for all samples made by normal sintering of powders C and F and hot

pressing of powders C. The correlation between the Curie temperature and axial ratio is observed; the coefficients of correlation were 0.76, 0.60, 0.62, and 0.60 for the samples with $x = 0.50$, 0.41, 0.37, and 0.30, respectively. The variation in the axial ratio indicates the presence of homogeneous strain in the samples.²⁰ The strain is caused by internal stresses, and the magnitude of strain is proportional to the magnitude of stresses. The correlation shown in Fig. 11 indicates that the variation in the Curie temperature is related to internal stresses.

Further evidence for the presence of internal stresses was obtained from the direct measurement of internal stresses by the microindentation method.¹⁵ To measure the magnitude of internal stresses, another set of samples was prepared by normal sintering and hot pressing. The sample made by normal sintering was fired at 1300°C for 1 h. For hot pressing, the pressure of 42 MPa was applied when the temperature reached a desired temperatures, 1220° and 1250°C. The samples hot pressed at 1250° were further annealed at 1275° and 1300°C to grow grains. Figure 12 shows examples of K_{1c} vs $c^{1/2}$ plot for the samples with $x = 0.50$ obtained under the various conditions. The linear relationship indicates that internal stresses can be evaluated from this plot. Figure 13 shows the relationship between the magnitude of internal stresses and the Curie temperature. A good correlation was obtained. This result indicates that the variation in the Curie temperature is caused by internal stresses.

(5) Effect of Composition on the Curie Temperature Variation

The paraelectric phase of $\text{Pb}_{1-x}\text{Ba}_x\text{Nb}_2\text{O}_6$ is tetragonal, and the ferroelectric phases in the samples with $x > 0.37$ and $x <$

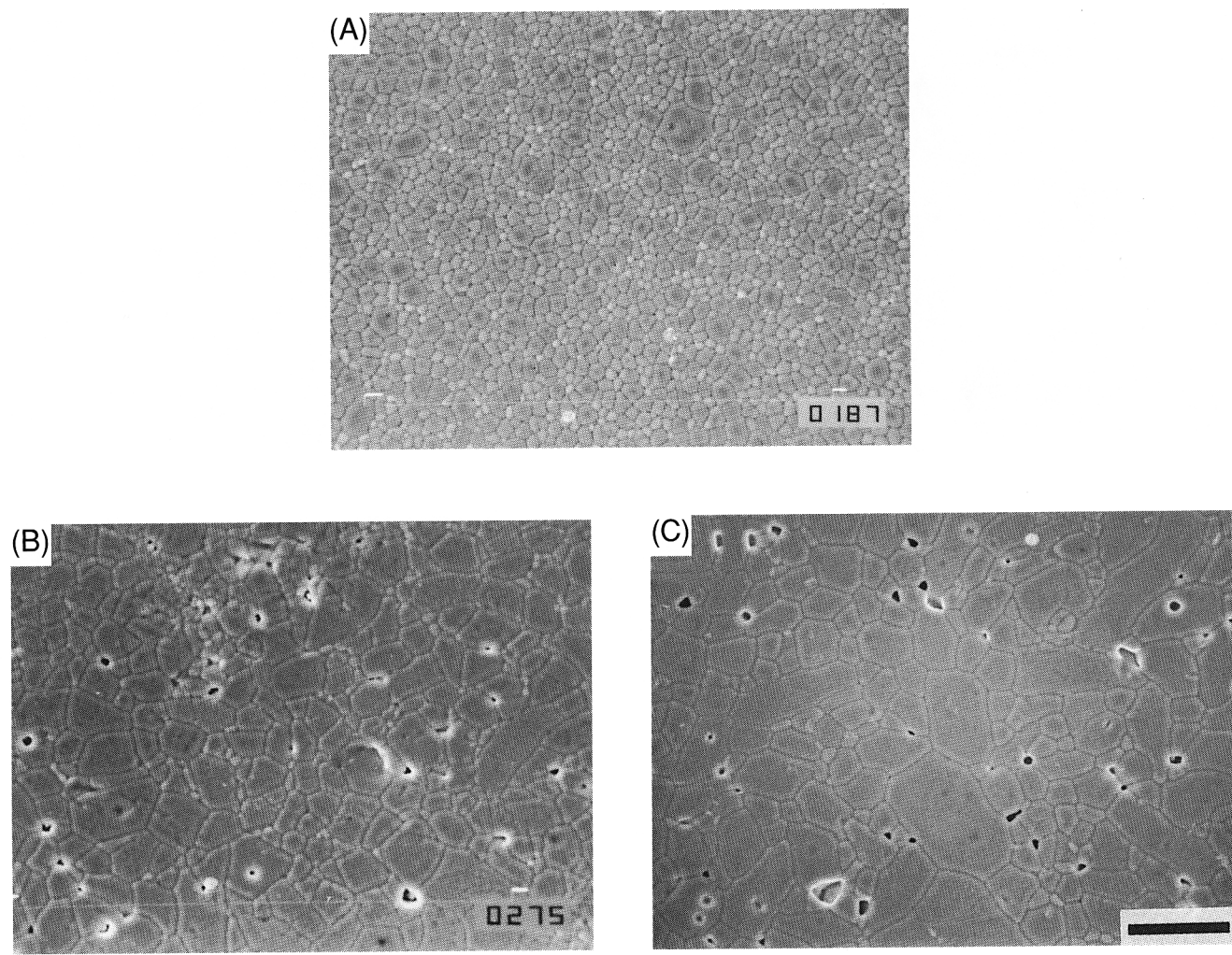


Fig. 6. Microstructures of the samples with $x = 0.50$ made by hot pressing of powder C by programs (A) I, (B) II, and (C) III (bar = 20 μm).

0.37 are tetragonal and orthorhombic, respectively.¹² For the transition to the tetragonal structure, only 180° domains form,⁸ and the relaxation of internal stresses by the formation of 90° domains is not possible. For the transition to the orthorhombic structure, however, 90° domains form,⁸ and the relaxation of internal stresses by the formation of 90° domains is

possible. Thus, it is expected that the tetragonal structure in the ferroelectric phase has larger internal stresses than the orthorhombic structure.

Because the magnitude of internal stresses is correlated to the variation in the Curie temperature as shown in Fig. 13, the

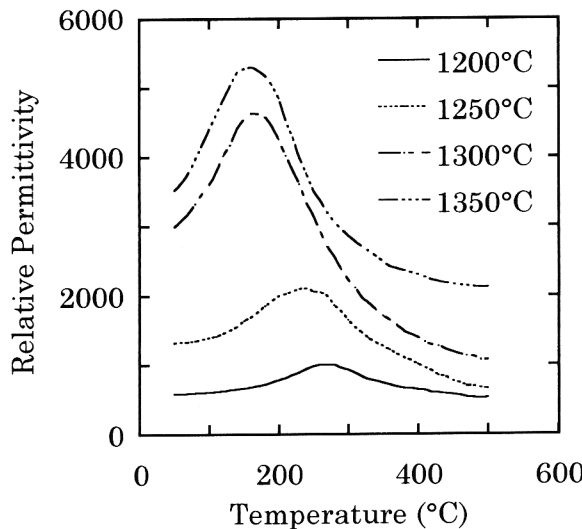


Fig. 7. Temperature dependence of relative permittivity of the samples with $x = 0.50$ made by normal sintering of powder C.

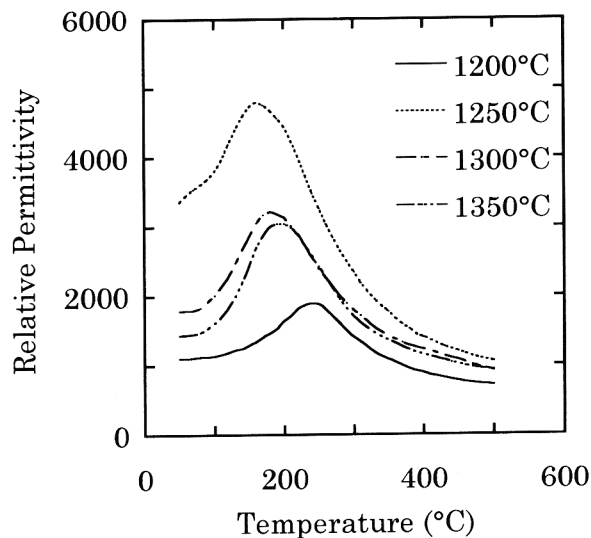


Fig. 8. Temperature dependence of relative permittivity of the samples with $x = 0.50$ made by normal sintering of powder F.

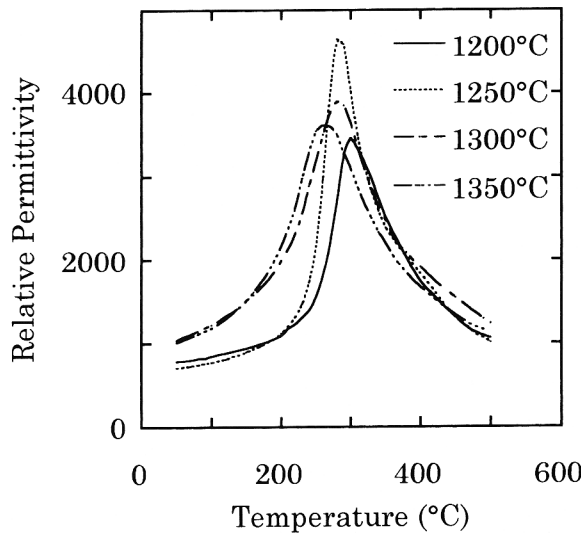


Fig. 9. Temperature dependence of relative permittivity of the samples with $x = 0.30$ made by normal sintering of powder F.

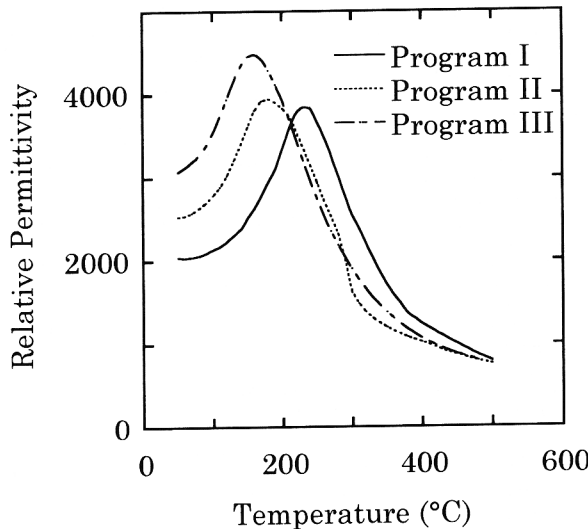


Fig. 10. Temperature dependence of relative permittivity of the samples with $x = 0.50$ obtained by hot pressing of powder C.

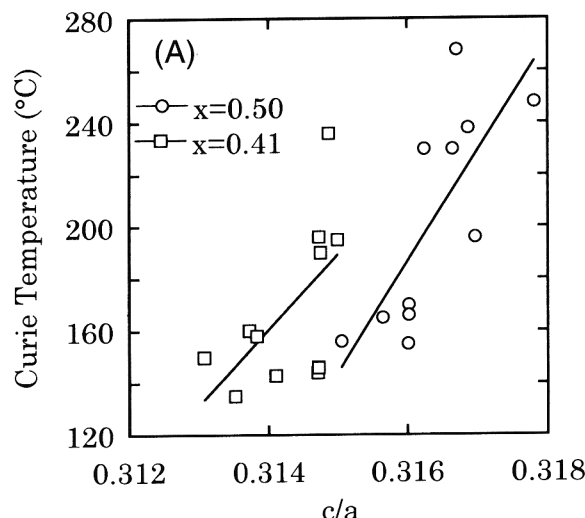


Fig. 11. Relation between the Curie temperature and axial ratio (A) c/a for the samples with $x = 0.41$ and 0.50 and (B) b/a for the samples with $x = 0.30$ and 0.37.

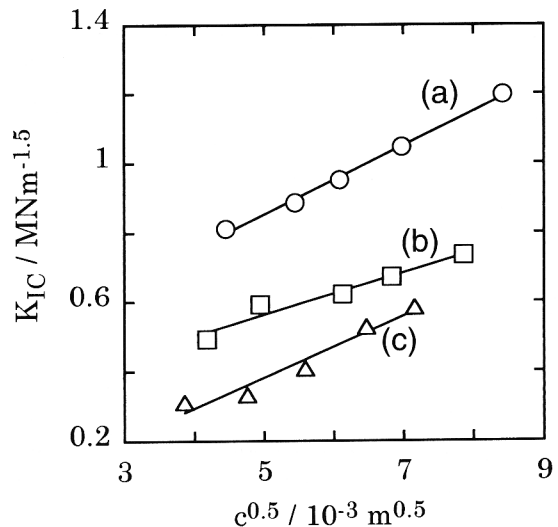


Fig. 12. Relation between $c^{0.5}$ and K_{IC} for the samples (a) hot pressed at 1250°C, (b) normally sintered at 1300°C, and (c) annealed of sample (a) at 1300°C.

effect of crystal structure of the ferroelectric phase is examined from the variation in the Curie temperature. The degree of the variation in the Curie temperature was obtained from the maximum and minimum Curie temperatures for the samples with the same composition made under the different conditions. The maximum and minimum Curie temperatures (T_{\max} and T_{\min} , respectively) were selected from the Curie temperatures of all samples with the same composition made by normal sintering and hot pressing of powders C and F (Fig. 11). The temperature difference, $T_{\max} - T_{\min}$, is the amount of the Curie temperature variation. Table I shows the maximum and minimum Curie temperatures and the Curie temperature variation. The amount of the Curie temperature variation was larger for $x = 0.41$ and 0.50 than for $x = 0.30$ and 0.37, indicating that larger internal stresses develop in the tetragonal ferroelectric phase than in the orthorhombic ferroelectric phase.

The direct measurement of the magnitude of internal stresses gave further evidence of the effect of crystal structure of ferroelectric phase on the development of internal stresses. The magnitude of internal stresses ranged from 54 to 87 MPa for the samples with $x = 0.50$, as shown in Fig. 13. The magnitude for the samples with $x = 0.37$ ranged from 46 to 52 MPa. The small values for the samples with $x = 0.37$ indicate that internal

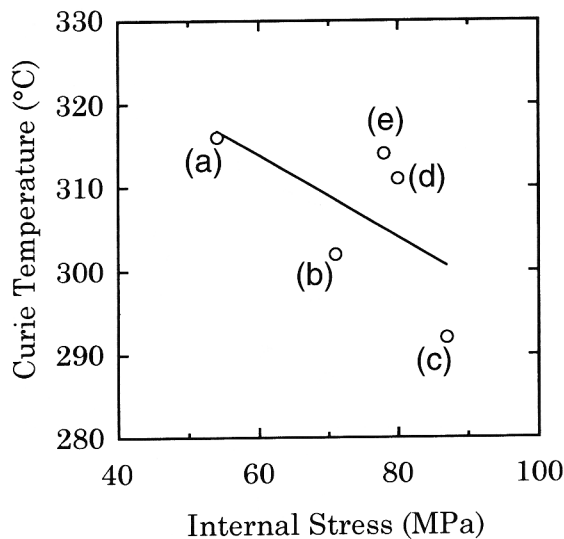


Fig. 13. Relation between internal stresses and the Curie temperature for the samples (a) normally sintered at 1300°C, (b) and (c) hot pressed at 1220° and 1250°C respectively, and (d) and (e) annealed of sample (c) at 1275° and 1300°C, respectively.

stresses were small for the ferroelectric phase with the orthorhombic structure.

IV. Conclusions

The effects of microstructure and composition on the Curie temperature were studied for $\text{Pb}_{1-x}\text{Ba}_x\text{Nb}_2\text{O}_6$ with $x = 0.30, 0.37, 0.41$, and 0.50 . The Curie temperature was dependent on the density and grain size of the polycrystalline samples, for which the development of internal stresses by the paraelectric-to-ferroelectric phase transition was responsible. The magnitude of internal stresses determined the Curie temperature variation. Pores and cracks relaxed internal stresses; the samples with large amounts of pores and cracks had high Curie temperatures. Grain boundaries also relaxed internal stresses;

Table I. Relation between Composition (x) and T_{\max} , T_{\min} , and $T_{\max} - T_{\min}$ Values

x	T_{\max} (°C)	T_{\min} (°C)	$T_{\max} - T_{\min}$ (°C)
0.30	302	260	42
0.37	188	138	50
0.41	236	135	101
0.50	268	156	112

samples with small grains had high Curie temperatures. Furthermore, the magnitude of internal stresses was dependent on the crystal structure of the ferroelectric phases. Internal stresses were relaxed by the formation of 90° domains in the samples with the orthorhombic ferroelectric structure, whereas such relaxation did not occur in the samples with the tetragonal ferroelectric structure. Thus, the amount of the Curie temperature variation was larger for the samples with $x = 0.41$ and 0.50 than those with $x = 0.30$ and 0.37 .

References

- B. Jimenez, C. Alemany, J. Mendiola, and E. Maurer, "Phase Transitions in Ferroelectric Ceramics of the Type $\text{Sr}_{0.5}\text{Ba}_{0.5}\text{Nb}_2\text{O}_6$," *J. Phys. Chem. Solids*, **46** [12] 1383–86 (1985).
- J. Thorez and J. Ravez, "Influence of Degree of Cation Order on Dielectric Properties of Some Phases of Type 'Tetragonal Tungsten Bronze,'" *Rev. Chim. Miner.*, **24** [3] 288–94 (1987).
- T. Kimura, S. Miyamoto, and T. Yamaguchi, "Microstructure Development and Dielectric Properties of Potassium Strontium Niobate Ceramics," *J. Am. Ceram. Soc.*, **73** [1] 127–30 (1990).
- T. Kimura, S. Saiubol, and K. Nagata, "Effect of Grain Orientation on the Curie Temperature of $\text{KSr}_2\text{Nb}_3\text{O}_15$ Solid Solutions," *J. Ceram. Soc. Japan, Int. Ed.*, **103** [2] 132–37 (1995).
- G. Burns and D. F. O'Kane, "Transition Temperature Variations in Sodium Barium Niobate and Related Compositions," *Phys. Lett.*, **28A** [11] 776–77 (1969).
- R. Guo, A. S. Bhalla, G. Burns, and F. H. Dacol, "Studies of Annealing and Quenching of Strontium Barium Niobate (SBN) Single Crystals: A-Site Cation Ordering-Disordering Effect," *Ferroelectrics*, **93**, 397–405 (1989).
- W.-H. Huang, Z. Xu, and D. Viehland, "Structure-Property Relationships in Strontium Barium Niobate II. Quenching and Annealing Effects," *Philos. Mag.*, **71** [2] 219–29 (1995).
- C. A. Randall, R. Guo, A. S. Bhalla, and L. E. Cross, "Microstructure-Property Relations in Tungsten Bronze Lead Barium Niobate, $\text{Pb}_{1-x}\text{Ba}_x\text{Nb}_2\text{O}_6$," *J. Mater. Res.*, **6** [8] 1720–28 (1991).
- E. C. Subbarao, "X-ray Study of Phase Transitions in Ferroelectric PbNb_2O_6 and Related Materials," *J. Am. Ceram. Soc.*, **43** [9] 439–42 (1960).
- M. H. Francombe, "The Relation between Structure and Ferroelectricity in Lead Barium and Barium Strontium Niobates," *Acta Crystallogr.*, **13**, 131–40 (1960).
- W. R. Buessem, L. E. Cross, and A. K. Goswami, "Phenomenological Theory of High Permittivity in Fine-Grained Barium Titanate," *J. Am. Ceram. Soc.*, **49** [1] 33–36 (1966).
- R. Guo, A. S. Bhalla, C. A. Randall, Z. P. Chang, and L. E. Cross, "Polarization Mechanisms of Morphotropic Phase Boundary Lead Barium Niobate (PBN) Compositions," *J. Appl. Phys.*, **67** [3] 1453–60 (1990).
- S. Tashiro, N. Sasaki, Y. Tsuji, H. Igarashi, and K. Okazaki, "Sintering of Submicron Powders by Ball-Milling," *Jpn. J. Appl. Phys.*, **26** [Suppl. 26-2] 142–44 (1987).
- M. I. Mendelson, "Average Grain Size in Polycrystalline Ceramics," *J. Am. Ceram. Soc.*, **52** [8] 443–46 (1969).
- K. Okazaki, "Mechanical Behavior of Ferroelectric Ceramics," *Am. Ceram. Soc. Bull.*, **63** [9] 1150–52, 1157 (1984).
- J. A. Kuszyk and R. C. Bradt, "Influence of Grain Size on Effects of Thermal Expansion Anisotropy in MgTi_2O_5 ," *J. Am. Ceram. Soc.*, **56** [8] 420–23 (1973).
- J. Cleveland and R. C. Bradt, "Grain Size/Microcracking Relations for Pseudobrookite Oxides," *J. Am. Ceram. Soc.*, **61** [11–12] 478–81 (1978).
- R. W. Rice and R. C. Pohanka, "Grain-Size Dependence of Spontaneous Cracking in Ceramics," *J. Am. Ceram. Soc.*, **62** [11–12] 559–63 (1979).
- J. K. Vij, "Pressure, Temperature, and Frequency Dependence of the Dielectric Properties of Strontium Barium Niobate," *Phys. Status Solidi, A*, **74** [1] 225–32 (1982).
- B. D. Cullity, *Elements of X-ray Diffraction*, 2nd ed.; pp. 287–92. Addison-Wesley, London, 1978. □